Functional role of CCL5/RANTES for HCC progression during chronic liver disease

Antje Mohs[1], Nadine Kuttkat[1], Johanna Reißing[1], Henning Wolfgang Zimmermann[1], Roland Sonntag[1], Amanda Proudfoot[2], Sameh A. Youssef[3], Alain de Bruin[3,4], Francisco Javier Cubero[1,†], Christian Trautwein[1,*,†]

[1]Department of Internal Medicine III, University Hospital, RWTH Aachen, Aachen, Germany; [2]Merck Serono Geneva Research Centre, Case postale 54, chemin des Mines 9, Geneva CH-1211 20, Switzerland; [3]Dutch Molecular Pathology Center, Department of Pathobiology, Faculty of Veterinary Medicine, Utrecht University, Yalelaan 1, 3508 TB Utrecht, The Netherlands; [4]University Medical Center Groningen, Department of Pediatrics, University of Groningen, NL-9713 Groningen, The Netherlands

Background & Aims: During liver inflammation, triggering fibrogenesis and carcinogenesis immune cells play a pivotal role. In the present study we investigated the role of CCL5 in human and in murine models of chronic liver inflammation leading to hepatocellular carcinoma (HCC) development.

Methods: CCL5 expression and its receptors were studied in well-defined patients with chronic liver disease (CLD) and in two murine inflammation based HCC models. The role of CCL5 in inflammation, fibrosis, tumor initiation and progression was analyzed in different cell populations of $NEMO^{\Delta hepa}/CCL5^{-/-}$ animals and after bone marrow transplantation (BMT). For therapeutic intervention Evasin-4 was injected for 24 h or 8 weeks.

Results: In CLD patients, *CCL5* and its receptor *CCR5* are overexpressed – an observation confirmed in the $Mdr2^{-/-}$ and $NEMO^{\Delta hepa}$ model. CCL5 deletion in $NEMO^{\Delta hepa}$ mice diminished hepatocyte apoptosis, compensatory proliferation and fibrogenesis due to reduced immune cell infiltration. Especially, CD45+/ Ly6G+ granulocytes, CD45+/CD11b+/Gr1.1+/F4/80+ proinflammatory monocytes, CD4+ and CD8+ T cells were decreased. One year old $NEMO^{\Delta hepa}/CCL5^{-/-}$ mice displayed smaller and less malignant tumors, characterized by reduced proliferative capacity and less pronounced angiogenesis. We identified hematopoietic cells as the main source of CCL5, while CCL5 deficiency did not sensitise $NEMO^{\Delta hepa}$ hepatocytes towards TNFα induced apoptosis. Finally, therapeutic intervention with Evasin-4 over a period of 8 weeks ameliorated liver disease progression.

Conclusion: We identified an important role of CCL5 in human and functionally in mice with disease progression, especially HCC development. A novel approach to inhibit CCL5 *in vivo* thus appears encouraging for patients with CLD.

Lay summary: Our present study identifies the essential role of the chemoattractive cytokine CCL5 for liver disease progression and especially hepatocellular carcinoma development in men and mice. Finally, the inhibition of CCL5 appears to be encouraging for therapy of human chronic liver disease.

ELSEVIER

Introduction

Under physiological conditions the inflammatory response is a beneficial process to restore tissue injury and to protect against pathogenic causes. However, persistent liver damage triggers chronic inflammation leading to scar formation and enhances the susceptibility for cancer development [1]. Hepatocellular carcinoma (HCC) is the third leading cause of cancer-related death and the fifth most common solid tumor worldwide [2]. Most HCCs develop in the context of chronic liver inflammation [3–5]. However, the molecular and cellular mechanisms linking inflammation and end-stage HCC during chronic liver injury need to be better defined in order to develop new treatment targets.

The intrahepatic accumulation of immune cells, a feature of chronic liver disease (CLD), is coordinated by an orchestra of chemokines and cytokines, which are produced by infiltrating as well as resident liver cells [6]. Our group and others have identified CC-chemokine ligand 5 (CCL5) – originally described as RANTES – as a 7.5 kDa chemokine [7], which plays a crucial role in the inflammatory process [8]. CCL5 is expressed by platelets, macrophages, endothelial cells and hepatic stellate cells (HSCs) [9,10]. Upon binding to its seven transmembrane G-protein coupled receptors CCR1, CCR3 and CCR5, CCL5 mediates its effect on cell trafficking and activation on a range of immune cells including T cells, monocytes, basophils, eosinophils, natural killer (NK) cells, and dendritic cells (DC) [11].

Two different experimental approaches of liver fibrosis *in vivo* – the methionine and choline deficient diet (MCD) and the toxic carbon tetrachloride (CCl_4) – have demonstrated that CCL5 deletion results in reduced fibrogenesis due to a decrease in

Research Article

intrahepatic macrophages and T cells [8]. Moreover, *CCR1* and *CCR5* knockout mice are protected against fibrogenesis after bile duct ligation or CCl₄-induced liver fibrosis [12].

Despite the fact that genetic deletion or pharmacological inhibition of CCL5 receptors have shown promising results as a first step towards anti-fibrotic therapy in the clinic, the lack of evidence with respect to the role of CCL5 in inflammation-induced tumorigenesis is not yet clearly defined. Furthermore, $CCR5^{-/-}$ mice, but not $CCR1^{-/-}$ animals are partially protected against tumorigenesis in the *Mdr2* knockout model [13]. In contrast, $CCR1^{-/-}$ mice displayed a lower number of nodules and reduced tumor size but higher tumor incidence after diethylnitrosamine (DEN) challenge [14].

Thus, we aimed to investigate the expression of CCL5 and its receptors in patients suffering from CLD and correlated its expression with disease progression. To functionally study the relevance of this finding in inflammation-driven liver carcinogenesis we applied the $NEMO^{\Delta hepa}$ mouse, an experimental model characterized by increased hepatocyte apoptosis and compensatory proliferation, leading to chronic hepatitis, which triggers fibrosis and finally HCC, mimicking non-alcoholic steatohepatitis (NASH) and HCC development in human [15,16]. Furthermore, we evaluated the therapeutic implications of blocking CCL5 against inflammation-derived HCC using Evasin-4, a chemokine-binding protein derived from the common brown dog tick which has high affinity and neutralization capacity for CCL5 [17,18].

Materials and methods

Housing and establishment of the knockout mice

We generated mice carrying the loxP-site-flanked *NEMO/IKKγ* gene under the control of the Alb/AFP-Cre promotor/enhancer as previously described [15,16,19]. From $NEMO^{\Delta hepa}$ mice, we generated double knockout animals by crossing $NEMO^{\Delta hepa}$ with constitutive CCL5 deficient mice defined in a C57BL/6 background and purchased from the Jackson Laboratory (Bar Harbor, ME) [20]. Progression of liver disease was monitored in male mice, ranging from 8 to 52 weeks of age. FACS experiments were performed on 8- week-old male mice. Animals were maintained in the animal facility of the University Hospital, RWTH Aachen according to the German legal requirements.

Human liver samples

Human liver tissue was acquired either from biopsies for routine clinical purposes or explants of cirrhotic livers obtained during liver transplantation [21].

For details on methodology, please see Supplementary Material.

Results

Increased CCL5 expression correlates with liver disease progression in humans

To define the relevance of CCL5 in CLD, we investigated its mRNA expression in liver samples of healthy controls and a cohort of patients with different stages of liver disease ranging from mild to advanced liver fibrosis and cirrhosis. *CCL5* expression was significantly higher in diseased livers compared with healthy controls (Fig. 1A). Interestingly, *CCL5* mRNA expression correlated with fibrosis grade (Fig. 1B) and the stage of liver inflammation

(Fig. 1C). When different etiologies of CLD were compared steatotic patients showed significantly higher *CCL5* expression. However, *CCL5* was also elevated in livers of NASH and viral hepatitis patients compared with healthy controls (Supplementary Fig. 1).

Next we analyzed CCL5 protein expression in patients with advanced liver fibrosis (F4). Immunohistochemical staining revealed that CCL5 was exclusively detected in non-parenchymal cells (NPCs) whereas immunohistochemistry was negative in healthy controls (Fig. 1D). Additionally, we observed a significant upregulation of *CCR5* in CLD patients compared with healthy controls, whereas *CCR1* and CCR3 expression was unaffected (Fig. 1E). Altogether these results indicate that *CCL5* expression correlates with the stage of liver fibrosis and might be a useful marker for NASH patients.

Increased CCL5 and CCR5 expression in NEMO^Δhepa livers

Our analysis revealed that *CCL5* and *CCR5* expression is increased in patients with different etiologies. This expression pattern was further confirmed in a first model of experimental liver disease, where steatohepatitis and its progression lead to fibrosis and HCC development [15]. Disease progression in $NEMO^{\Delta hepa}$ animals mimics chronic inflammation and HCC in human; therefore it represents an excellent experimental model to study CLD. In $NEMO^{\Delta hepa}$ livers we observed a significant upregulation of *CCL5* and *CCR5* whereas the expression of *CCR1* and *CCR3* remained unchanged compared with wild-type (WT) mice (Fig. 2A; Supplementary Fig. 2A). Furthermore we found an upregulation of *CCL5* in the non-immune cell fraction (including HSCs and hepatocytes) as well as in the immune cell fraction in $NEMO^{\Delta hepa}$ livers compared to WT livers. However, the immune cell fraction showed a significant higher *CCL5* expression compared to the non-immune cell fraction in $NEMO^{\Delta hepa}$ livers (Supplementary Fig. 2B).

To further strengthen the relevance of our findings, we investigated expression of *CCL5* and its receptors in a second example of inflammation triggered chronic liver injury, the $Mdr2^{-/-}$ model. Here we found higher *CCL5* expression, while the receptors *CCR1*, *CCR3* and *CCR5* remained unchanged compared with WT livers (Supplementary Fig. 2C).

To study CCR1 and CCR5 expression in liver cells, we isolated immune and non-immune cells from WT and $NEMO^{\Delta hepa}$ livers. On the mRNA level, both cell fractions from $NEMO^{\Delta hepa}$ compared with WT livers showed higher *CCR5* expression. In addition, in $NEMO^{\Delta hepa}$ immune cells *CCR1* expression was significantly upregulated (Fig. 2B). To characterize CCR1 and CCR5 expression on the protein level we next performed FACS analysis and immunofluorescence staining. Here we found an increase in absolute numbers of CD45⁺/CCR5⁺ cells in $NEMO^{\Delta hepa}$ compared to WT livers (Fig. 2C). Additionally, we could show that CCR5 surface expression was increased on Ly6G⁺, CD11b⁺/F40/80⁺/GR1.1⁺ cells in $NEMO^{\Delta hepa}$ compared to WT livers. Characteristically, the percentage of Ly6G⁺, CD11b⁺/F40/80⁺/GR1.1⁺ and CD3⁺ cells expressing CCR5 was upregulated in $NEMO^{\Delta hepa}$ livers as compared to WT livers (Supplementary Fig. 3A and B).

Interestingly, $NEMO^{\Delta hepa}$ mice show CCL5 and CCR5 upregulation as also found in patients with CLD and our results further identify immune cells to be responsible in mediating this effect.
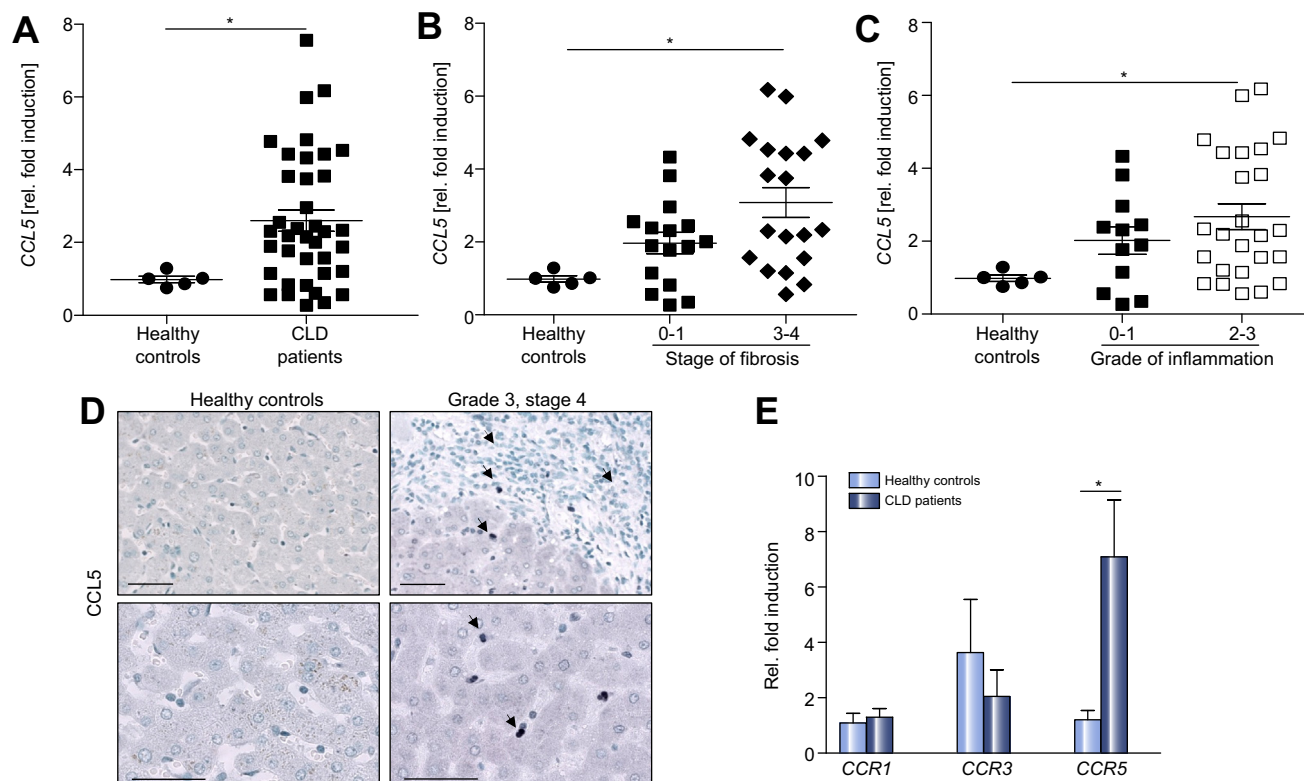
Fig. 1. CCL5 overexpression is a common pattern of human CLD. Total RNA was extracted from liver samples of healthy controls and CLD patients. Expression level of *CCL5*, *CCR1*, *CCR3* and *CCR5* were measured by qRT-PCR. (A) *CCL5* expression of CLD patients (n = 41) in comparison with healthy controls (n = 5). (B) *CCL5* expression of CLD patients with different fibrosis stages (stage 0–1: n = 16; stage 3–4 n = 19) in comparison with healthy controls (n = 5). (C) *CCL5* expression of CLD patients with different stages of inflammation (stage 0–1: n = 12; stage 2–3: n = 25) in comparison with healthy controls. (D) Representative CCL5 immunohistochemical staining of paraffin embedded liver samples of a healthy control and a CLD patient. Arrows indicate positive cells. Scale bar: 50 μm. (E) Expression of *CCR1*, *CCR3* and *CCR5* in CLD patients compared (n = 28) with healthy controls (n = 5). Data are expressed as mean ± SEM. Statistical differences were detected by one-way ANOVA with Tukey's post-hoc (B, C) and by a 2-tailed Student's *t* test (A, E) (*p <0.05).

CCL5 deletion significantly improves liver injury in NEMO$^{\Delta hepa}$ mice

Our human data indicated a role for the CCL5/CCR5 axis during CLD. Results in the NEMO$^{\Delta hepa}$ livers best reflected these observations, we thus generated NEMO$^{\Delta hepa}$/CCL5$^{-/-}$ mice to study the impact of constitutive *CCL5* deletion on disease progression. H&E staining of 8 week old NEMO$^{\Delta hepa}$ livers revealed signs of lobular disorganization and severe diffuse hepatocellular aniso-karyosis together with increased apoptotic and mitosis accompanied by mild inflammation. In contrast, NEMO$^{\Delta hepa}$/CCL5$^{-/-}$ displayed less pronounced liver damage (Fig. 2D; Supplementary Fig. 4A), which was also reflected in a significant reduction in serum alanine transaminases (ALT) values at all investigated time points (Supplementary Fig. 4F).

We now verified the effect of *CCL5* deletion on apoptosis and compensatory proliferation in NEMO$^{\Delta hepa}$ and NEMO$^{\Delta hepa}$/CCL5$^{-/-}$ livers. NEMO$^{\Delta hepa}$ mice displayed significantly more apoptosis than NEMO$^{\Delta hepa}$/CCL5$^{-/-}$ mice, as illustrated by higher numbers of cleaved caspase 3 positive cells, higher caspase 3 activity (Fig. 2D and E; Supplementary Fig. 4A and B) and increased TUNEL positive cells (Supplementary Fig. 4C and D). Immunofluorescence staining for Ki67 as well as expression analysis of key cell cycle markers (Fig. 2D–F; Supplementary Fig. 4E) showed a significant reduction in proliferation in 8 week old NEMO$^{\Delta hepa}$/CCL5$^{-/-}$ livers.

Loss of CCL5 alters the inflammatory milieu and the recruitment of immune cells

CCL5 plays a crucial role in recruiting a variety of leukocytes into inflammatory sites including macrophages, eosinophils, basophils and T cells [11]. The pro-inflammatory milieu in NEMO$^{\Delta hepa}$/CCL5$^{-/-}$ livers was attenuated compared with NEMO$^{\Delta hepa}$ livers as reflected by decreased *TNFα, IL-1β* and *MCP-1* expression levels (Fig. 3A). As shown for TNFα these results were confirmed by ELISA in whole liver tissue lysates (Fig. 3B).

No differences in intrahepatic immune cell infiltration were found between WT and *CCL5*$^{-/-}$ livers. However less infiltrating CD45$^+$ cells were observed in NEMO$^{\Delta hepa}$/CCL5$^{-/-}$ compared with NEMO$^{\Delta hepa}$ livers (Fig. 3C and F). Indeed, analysis of the number of intrahepatic immune cells revealed differences in specific subsets. Pro-inflammatory monocytes, defined as CD11b$^+$, Gr1.1$^+$ and F4/80$^+$, were significantly decreased in NEMO$^{\Delta hepa}$/CCL5$^{-/-}$ compared with NEMO$^{\Delta hepa}$ livers (Fig. 3D and F; Supplementary Fig. 5A). Moreover, the number of Ly6G$^+$ granulocytes was also lower in NEMO$^{\Delta hepa}$/CCL5$^{-/-}$ livers (Fig. 3E and F; Supplementary Fig. 5A), suggesting a reduced recruitment of innate immune cells. Additionally, the number of adaptive immune cells – CD4$^+$ and CD8$^+$ T cells – was diminished in NEMO$^{\Delta hepa}$/CCL5$^{-/-}$ livers (Supplementary Fig. 5C and D), while CD11c$^+$/b$^+$, CD11c$^+$/b$^-$

Cancer
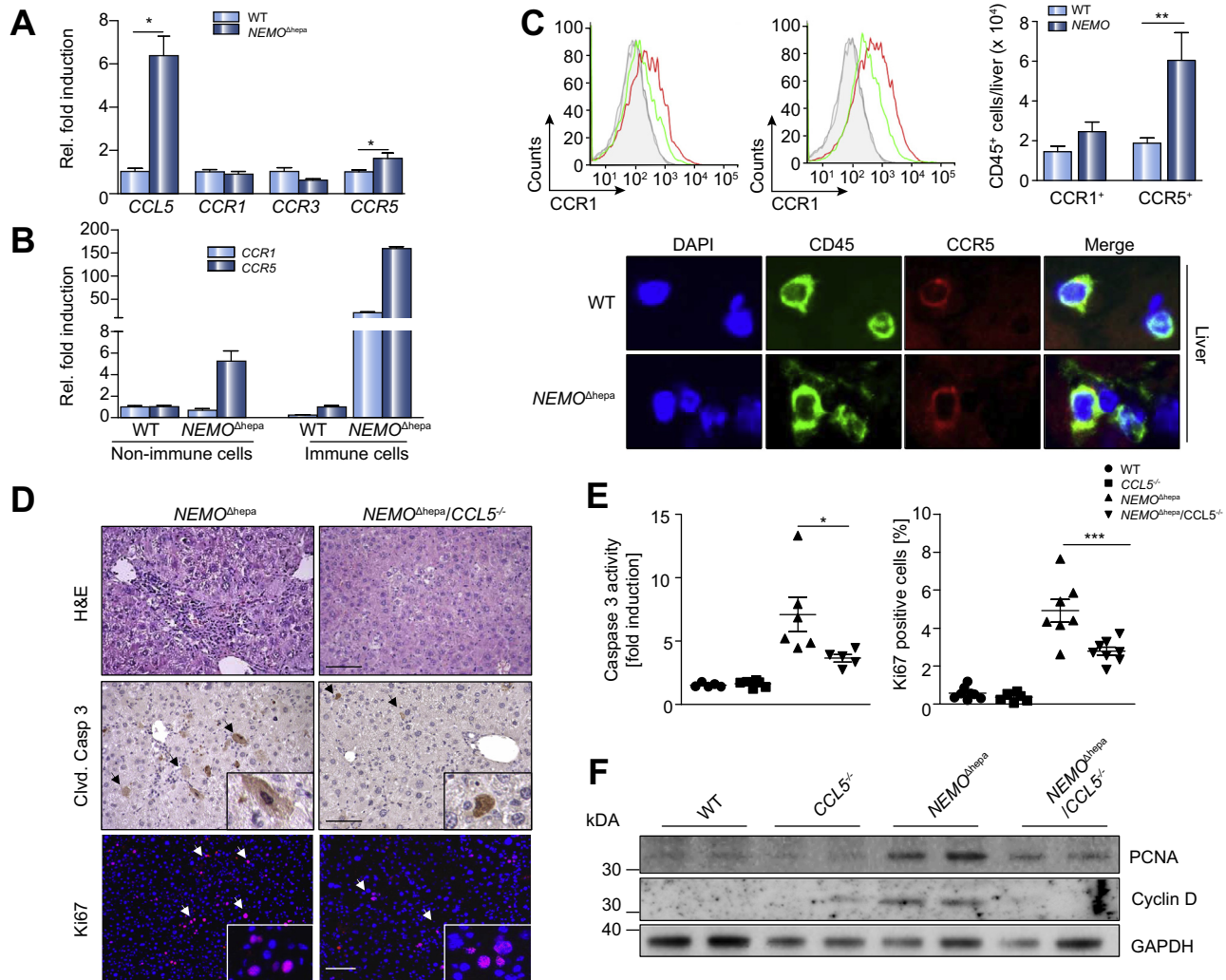
Fig. 2. Ablation of CCL5 in *NEMO*^Δhepa livers results in reduced liver injury. Samples of 8 week old WT, *CCL5*^−/−, *NEMO*^Δhepa and *NEMO*^Δhepa/*CCL5*^−/− mice were included. (A) Expression of *CCL5*, *CCR1*, *CCR3* and *CCR5* were measured by qRT-PCR in whole liver and presented as fold induction compared with WT mice. (B) Immune and non-immune cells from 8 week old WT and *NEMO*^Δhepa mice were isolated and *CCR1* and *CCR5* expression was quantified by qRT-PCR and presented as fold induction compared to WT immune or non-immune cells. (C) WT and *NEMO*^Δhepa liver immune cells were isolated and stained for CD45, CCR1 and CCR5. Representative histograms showing CCR1 and CCR5 expression on hepatic immune cells (gated on CD45^+, Hoechst^−) are shown. The absolute number of CD45^+/CCR1^+ and CD45^+/CCR5^+ cells was quantified. Liver sections were stained for CD45 to identify immune cells (green), CCR5 (red) and nuclei were counterstained with DAPI (blue). (D) Representative images of H&E (top), Clvd. caspase 3 (middle) and Ki67 (bottom) stained sections. Nuclei were counterstained with DAPI. Arrows indicate positive cells. Scale bar: 100 μm. (E) Caspase 3 activity was determined in whole liver extracts. Activities were calculated as fold induction compared with WT mice (left panel). Quantification of Ki67 positive cells was performed by using Image J (right panel). (F) Immunoblot analysis from whole liver extracts of cell cycle markers (PCNA, Cyclin D) and GAPDH as loading control. Data are expressed as mean ± SEM from 5 to 7 mice per group. Statistical differences were detected by one-way ANOVA with Tukey's post-hoc ($^*p$ <0.05; $^{**}p$ <0.01; $^{***}p$ = 0.001).

DCs or CD19^+ B cells were not affected (Supplementary Fig. 5E and F).

NEMO^Δhepa/*CCL5*^−/− *livers display reduced fibrogenesis*

CCL5 deletion significantly reduced the inflammatory response in 8 week old *NEMO*^Δhepa livers. As chronic inflammation triggers scar formation, we first investigated the impact on liver fibrogenesis. *NEMO*^Δhepa/*CCL5*^−/− livers exhibited diminished collagen deposition, as detected by decreased Sirius Red and collagen IA1 staining compared with *NEMO*^Δhepa mice (Fig. 4A and B). These results were further confirmed by collagen IA1 immunoblotting (Fig. 4C). Moreover, liver *TGFβ* mRNA expression levels as profi-

brotic cytokine were significantly downregulated in *NEMO*^Δhepa/*CCL5*^−/− compared with *NEMO*^Δhepa mice (Fig. 4D). Thus the attenuated inflammatory response in *NEMO*^Δhepa/*CCL5*^−/− livers was associated over time with reduced fibrogenesis.

Genetic CCL5 deletion diminishes HCC progression but not initiation

In total, 100% of one year old *NEMO* mice develop HCCs [22]. Thus, we assessed the impact of *CCL5* deletion on liver carcinogenesis. Macroscopically, tumors could be detected on the surface of *NEMO*^Δhepa and *NEMO*^Δhepa/*CCL5*^−/− livers (Fig. 5A; Supplementary Fig. 6A). However, the average largest tumor in *NEMO*^Δhepa/*CCL5*^−/− livers was significantly smaller compared
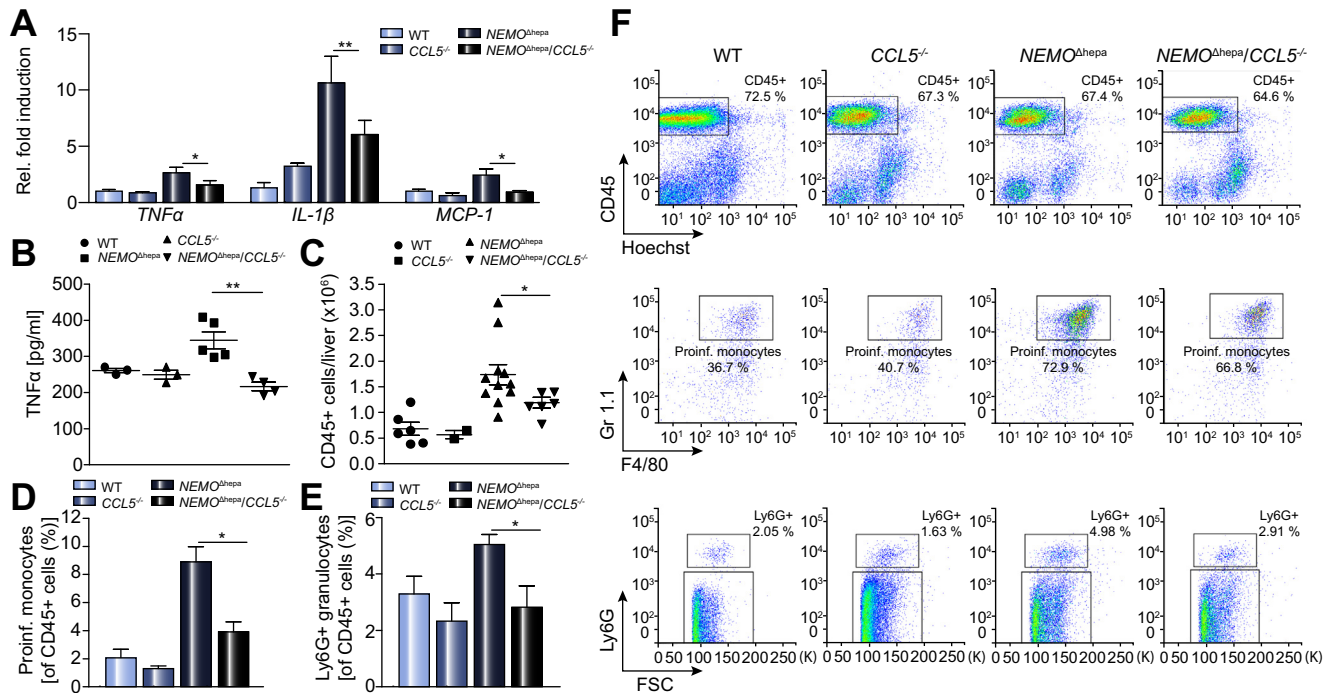
Fig. 3. Immune cell infiltration and inflammation status in NEMO$^{\Delta hepa}$/CCL5$^{-/-}$ mice. Samples of 8 week old WT, CCL5$^{-/-}$, NEMO$^{\Delta hepa}$ and NEMO$^{\Delta hepa}$/CCL5$^{-/-}$ mice were included. (A) Expression of TNFα, IL-1β and MCP-1 were measured by qRT-PCR in whole liver extracts and presented as fold induction compared with WT mice. (B) ELISA for TNFα of whole liver extracts from 8 week old mice was performed. (C) Absolute number of CD45$^+$ cells in the liver was calculated by using FlowJo. (D) Quantification of pro-inflammatory monocytes (Gr1.1$^+$/F4/80$^+$) and (E) Ly6G$^+$ granulocytes of CD45$^+$ cells was done using FlowJo. (F) Representative FACS plots from all four genotypes (WT, CCL5$^{-/-}$, NEMO$^{\Delta hepa}$ and NEMO$^{\Delta hepa}$/CCL5$^{-/-}$) for CD45$^+$ cells, Gr1.1$^+$/F4/80$^+$ proinf. Monocytes and Ly6G$^+$ granulocytes are shown. Data are expressed as mean ± SEM from 6 to 11 mice per group. Statistical differences were detected by one-way ANOVA with Tukey's post-hoc ($^*p$ <0.05; $^{**}p$ <0.01).

with the average largest tumor in NEMO$^{\Delta hepa}$ livers (Fig. 5B). H&E staining revealed that NEMO$^{\Delta hepa}$ livers exhibited single or multiple well-differentiated grade I trabecular HCC, whereas NEMO$^{\Delta hepa}$/CCL5$^{-/-}$ livers exhibited less neoplastic severity, supported by a decreased HCC incidence and a significantly less malignancy atypia score, characterized by variations in size or morphology of cells and of bizarre mitotic figures (Fig. 5C). In agreement, serum ALT and AP levels were significantly decreased in 1 year old NEMO$^{\Delta hepa}$/CCL5$^{-/-}$ compared with NEMO$^{\Delta hepa}$ mice (Supplementary Fig. 6A).

The proliferative capacity of the tumors as well as of non-neoplastic lesions was investigated in NEMO$^{\Delta hepa}$ and NEMO$^{\Delta hepa}$/CCL5$^{-/-}$ livers. Ki67 immunohistochemistry staining (Fig. 5A and D) demonstrated that non-neoplastic lesions exhibited reduced proliferation. Detailed analysis of the tumor tissue revealed a significant lower number of Ki67 positive hepatocytes and NPCs in NEMO$^{\Delta hepa}$/CCL5$^{-/-}$ compared with NEMO$^{\Delta hepa}$ tumor tissue (Supplementary Fig. 6C). Detailed analysis of cell cycle markers supported the concept that NEMO$^{\Delta hepa}$/CCL5$^{-/-}$ livers tumors showed a reduced proliferating capacity (Supplementary Fig. 6D).

Vessel formation from pre-existing vessels is an important feature of tumor formation to provide the tumor tissue with nutrient supply, essential for survival of tumor cells [23]. VEGF is linked to tumor angiogenesis and is strongly increased in NEMO$^{\Delta hepa}$ tumors. In contrast, its expression was significantly reduced in NEMO$^{\Delta hepa}$/CCL5$^{-/-}$ tumors and not significantly higher compared to controls (Fig. 5E). Accordingly NEMO$^{\Delta hepa}$/CCL5$^{-/-}$ livers showed significantly reduced CD31-positive area

– a marker for endothelial cells - compared with NEMO$^{\Delta hepa}$ livers (Fig. 5E; Supplementary Fig. 6E). Double staining for Ki67 and CD31 excluded that endothelial cells are part of the proliferating cells in the tumors (Supplementary Fig. 7).

To address whether CCL5 may increase VEGF expression, an in vitro tube formation assay was performed using LX-2 and HepG2 cells. Both cell lines were stimulated for 24 h with CCL5 and VEGF expression was quantified. CCL5 triggered VEGF expression in a dose dependent manner. In the HSC line LX-2 stronger VEGF expression was found compared with HepG2 cells (Fig. 5F (left panel); Supplementary Fig. 6F). CCL5 stimulation of primary murine HSCs, but not of primary murine hepatocytes, resulted in increased VEGF expression (Supplementary Fig. 5G, data not shown). Stimulation of human umbilical vein endothelial cells (HUVECs) seeded in matrigel with LX-2 or HepG2 supernatant resulted in the formation of vessel like structures (Fig. 5F; Supplementary Fig. 6F). In agreement with higher VEGF stimulation the supernatant of LX-2 supernatant induced stronger formation of vessel like structures (Fig. 5F; Supplementary Fig. 6F).

Hence liver disease progression and thus HCC malignant growth was significantly reduced in NEMO$^{\Delta hepa}$ mice after CCL5 deletion.

Deletion of CCL5 in NEMO$^{\Delta hepa}$ hepatocytes does not alter its viability and sensitivity after TNF stimulation

We next aimed to better define the cells and molecular mechanism explaining the protective effect of CCL5. We isolated primary hepatocytes from WT, CCL5$^{-/-}$, NEMO$^{\Delta hepa}$ and

Cancer
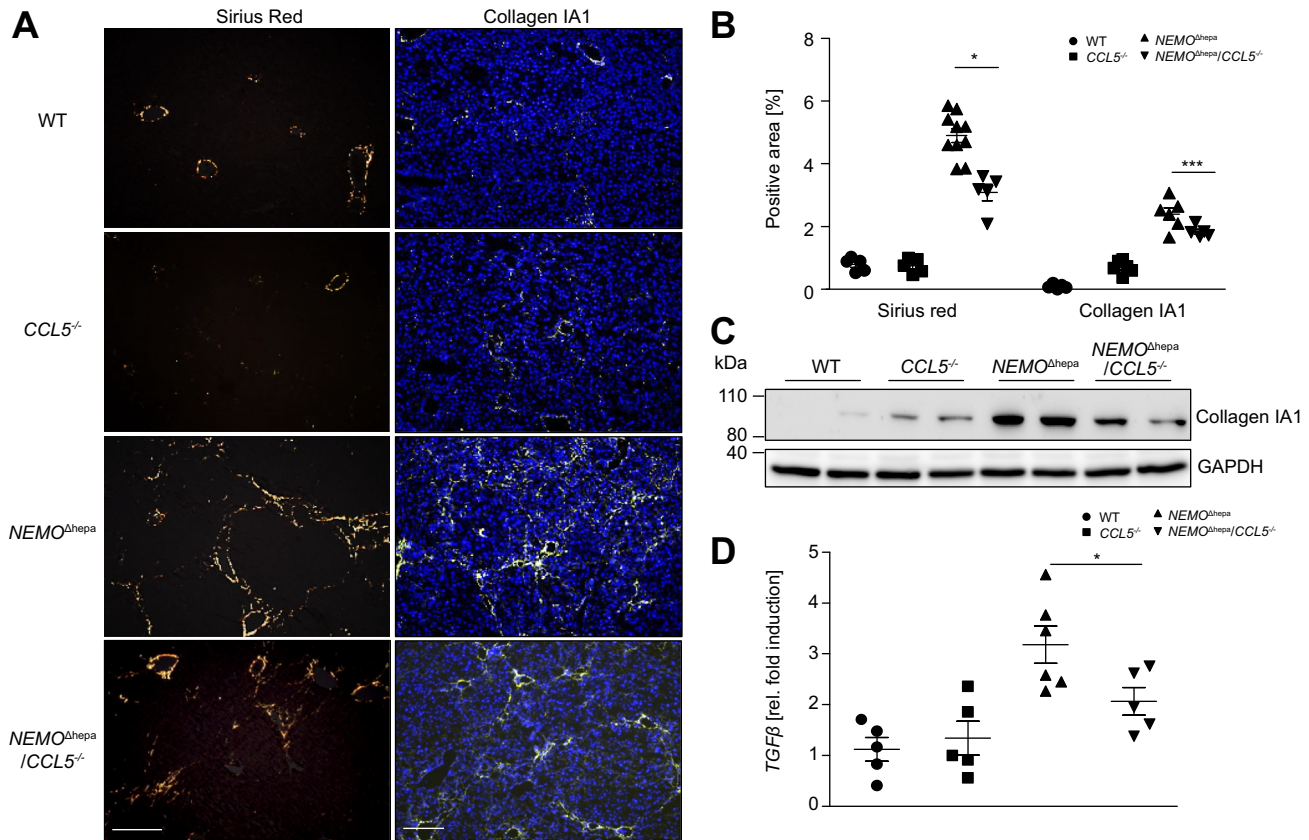
Fig. 4. Deletion of *CCL5* in *NEMO*^{Δhepa} liver ameliorates liver fibrosis. Samples of 13 week old WT, *CCL5*$^{-/-}$, *NEMO*$^{\Delta hepa}$ and *NEMO*$^{\Delta hepa}$/*CCL5*$^{-/-}$ mice were included. (A) Representative images of Sirius Red (left) and Collagen IA1 (right) stained sections. Nuclei were counterstained with DAPI. Scale bar: 200 μm. (B) Quantification of Sirius Red and Collagen IA1 positive area was performed using Image J. (C) Immunoblot analysis of whole liver extracts from 13 week old mice using antibodies against Collagen IA1 and GAPDH as loading control. (D) *TGFβ* expression level was measured by qRT-PCR in whole liver and presented as fold induction compared with WT mice. Data are expressed as mean ± SEM from 5 to 14 mice per group. Statistical differences were detected by one-way ANOVA with Tukey's post-hoc (*p <0.05).

NEMO$^{\Delta hepa}$/*CCL5*$^{-/-}$ animals. Viability after hepatocyte isolation from *NEMO*$^{\Delta hepa}$ and *NEMO*$^{\Delta hepa}$/*CCL5*$^{-/-}$ livers was significantly reduced compared with WT, *CCL5*$^{-/-}$ livers. Additionally there was significantly reduced viability of *NEMO*$^{\Delta hepa}$ compared with *NEMO*$^{\Delta hepa}$/*CCL5*$^{-/-}$ hepatocytes (Supplementary Fig. 8A).

As described earlier, *NEMO*$^{\Delta hepa}$ hepatocytes are sensitive to TNFα induced apoptosis *in vitro* and *in vivo* [19]. In contrast to the differences found after isolation, viability in culture over time was not different between *NEMO*$^{\Delta hepa}$ and *NEMO*$^{\Delta hepa}$/*CCL5*$^{-/-}$ hepatocytes. Additionally, hepatocytes derived from both genotypes are sensitive towards TNFα stimulation, however no differences were found between *NEMO*$^{\Delta hepa}$ and *NEMO*$^{\Delta hepa}$/*CCL5*$^{-/-}$ hepatocytes as evidenced by no changes in ALT levels, caspase 3 activity and corresponding images (Supplementary Fig. 8B–D).

Hematopoietic-derived CCL5 strongly influences the development of liver fibrosis

Our human data revealed that predominantly NPCs were CCL5 positive in CLD. Immune cells, including T cells, macrophages as well as resident liver cells (endothelial cells and HSCs) produce CCL5 [4–6]. To define if CCL5 of infiltrating immune cells or other NPCs are essential in determining CLD progression, we generated chimeric mice using bone marrow transplantation (BMT) (Fig. 6A).

Eight weeks after BMT, [WT→WT] and [*CCL5*$^{-/-}$→WT] chimeras displayed no significant differences in serum transaminases (Fig. 6B) or in hepatic fibrogenesis (Fig. 6C–E). Interestingly, [*CCL5*$^{-/-}$→*NEMO*$^{\Delta hepa}$] showed significantly lower AST and ALT values compared with chimeric [WT→*NEMO*$^{\Delta hepa}$] mice whereas [WT→*NEMO*$^{\Delta hepa}$/*CCL5*$^{-/-}$] mice displayed no differences compared to [WT→*NEMO*$^{\Delta hepa}$] mice (Fig. 6B). Concomitant with these findings, the H&E staining manifested a preserved hepatic architecture in [*CCL5*$^{-/-}$→*NEMO*$^{\Delta hepa}$] compared with [WT→*NEMO*$^{\Delta hepa}$] and [WT→*NEMO*$^{\Delta hepa}$/*CCL5*$^{-/-}$] livers (Fig. 6C). Moreover, the analysis of fibrosis markers such as collagen IA1, Sirius Red and TGFβ confirmed significantly decreased matrix deposition in [*CCL5*$^{-/-}$→*NEMO*$^{\Delta hepa}$] chimeras compared to [WT→*NEMO*$^{\Delta hepa}$] livers and [WT→*NEMO*$^{\Delta hepa}$/*CCL5*$^{-/-}$] (Fig. 6C–E). These results demonstrate that *CCL5* knockout in resident liver cells is insufficient for fibrosis improvement. In contrast, depletion of bone marrow derived-CCL5 significantly improved liver disease progression in *NEMO*$^{\Delta hepa}$ mice.

*Evasin-4 prevents the development of hepatic fibrosis in vivo*

Evasin-4 is a chemokine-binding protein, originally cloned from a cDNA library derived from the salivary glands of the common brown dog tick. Since Evasin-4 presents the highest binding affinity to CCL5 [17,18,24], we assessed if Evasin-4 treatment
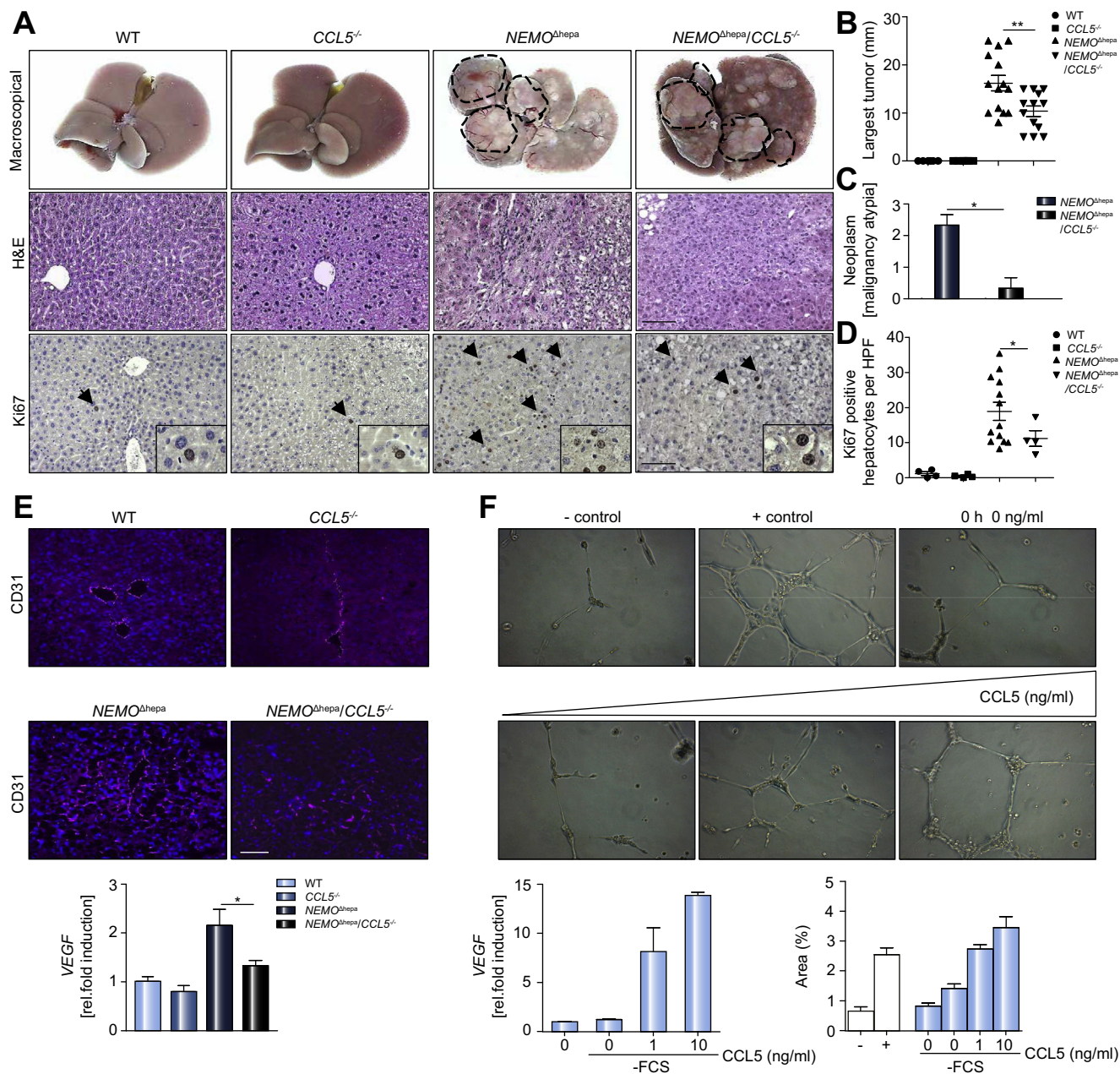
Fig. 5. Loss of *CCL5* in *NEMO*$^{\Delta hepa}$ livers attenuates HCC progression. Samples of 52 week old WT, *CCL5*$^{-/-}$, *NEMO*$^{\Delta hepa}$ and *NEMO*$^{\Delta hepa}$/*CCL5*$^{-/-}$ mice were included. (A) Representative liver pictures of 52 week old livers (top). Dashed circles indicate tumors. Representative pictures of H&E and Ki67 stained sections. Nuclei were counterstained with DAPI. Arrows indicate positive cells. Scale bar: 100 μm. (B) Quantification of the largest tumor of *NEMO*$^{\Delta hepa}$ and *NEMO*$^{\Delta hepa}$/*CCL5*$^{-/-}$ mice was performed using Image J. (C) Malignancy atypia scoring was performed by a pathologist of H&E stained paraffin embedded liver samples. (D) Quantification of Ki67 positive cells was performed using Image J. (E) Representative images of CD31 stained sections. Nuclei were counterstained with DAPI. Scale bar: 100 μm. *VEGF* expression level was measured by qRT-PCR in whole liver and tumor tissue and presented as fold induction compared with WT mice. Data are expressed as mean ± SEM from 6 to 14 mice per group. Statistical differences were detected by one-way ANOVA with Tukey's post-hoc (B, D, E) and by a 2-tailed Student's *t* test (C) (*$p < 0.05$; **$p < 0.01$). (F) Tube formation assay. HUVECs, seeded in matrigel, were stimulated 12 h with supernatant of LX-2 cells treated with CCL5 (0, 1 and 10 ng/ml). *VEGF* expression level in LX-2 cells was measured by qRT-PCR and presented as fold induction compared to control LX-2 cells (0 h, 0 ng/ml CCL5). Quantification of vessel-positive areas was performed by Image J.

influences early immune cell infiltration into the liver. Therefore, we injected Evasin-4 intraperitoneally in *NEMO*$^{\Delta hepa}$ mice at 8 weeks and sacrificed the mice after 24 h (Fig. 7A). CD45$^+$/Ly6G$^+$ granulocytes were significantly reduced in Evasin-4-treated-*NEMO*$^{\Delta hepa}$ mice compared with saline injected-*NEMO*$^{\Delta hepa}$ mice (Fig. 7B and C).

After we found that Evasin-4 reduced immune cell infiltration in *NEMO*$^{\Delta hepa}$ livers we injected Evasin-4 into *NEMO*$^{\Delta hepa}$ mice daily intraperitoneally over a period of 8 weeks (Fig. 7A) to address the question if Evasin-4 treatment could diminish fibrosis development. We evaluated markers of liver fibrosis and HSC activation, because *NEMO*$^{\Delta hepa}$ mice develop significant fibrosis
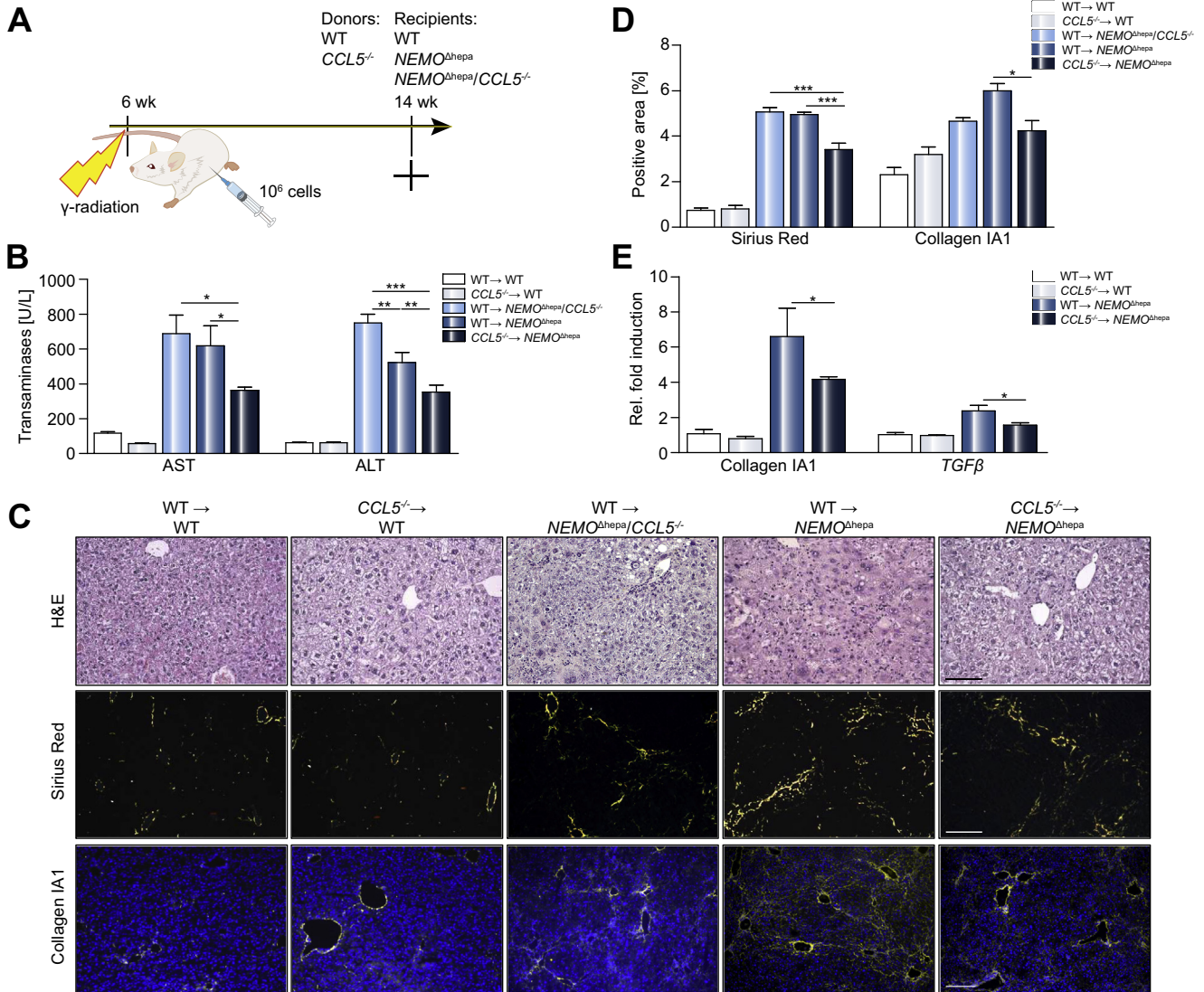
Fig. 6. Loss of hematopoietic CCL5 improves liver fibrogenesis in *NEMO*Δhepa mice. (A) Experimental setup. 6 week old WT and *NEMO*Δhepa mice were γ-irradiated and transplanted either with WT or with *CCL5*−/− bone marrow cells, as a control *NEMO*Δhepa/*CCL5*−/− received WT bone marrow cells. After 8 weeks mice were sacrificed and analyzed. Samples of WT mice transplanted with WT [WT → WT] or *CCL5*−/− [*CCL5*−/− → WT] and], *NEMO*Δhepa mice transplanted with WT [WT → *NEMO*Δhepa] or *CCL5*−/− [*CCL5*−/− → *NEMO*Δhepa] and *NEMO*Δhepa/*CCL5*−/− mice transplanted with WT [WT → *NEMO*Δhepa/*CCL5*−/−] were included in this analyzes. (B) Serum AST and ALT values were measured in all indicated groups. (C) Representative images of H&E (top) (Scale bar: 100 μm), Sirius Red (middle) and collagen IA1 (bottom) stained sections (Scale bar: 200 μm). Nuclei were counterstained with DAPI. (D) Quantification of Sirius Red and collagen IA1 positive area was performed using Image J. (E) Expression of collagen IA1 and *TGFβ* were measured by qRT-PCR in whole liver and presented as fold induction compared with [WT → WT]. Data are expressed as mean ± SEM from 7 to 10 mice per group. Statistical differences were detected by one-way ANOVA with Tukey's post-hoc (*p <0.05; **p <0.01; ***p = 0.001).

and matrix deposition and signs of NASH, between 13–14 weeks of age. Sirius Red staining and collagen IA1 staining revealed that Evasin-4-treated *NEMO*Δhepa mice displayed significant less fibrosis after 8 weeks of treatment (Fig. 7D and E). Our results were confirmed by quantitative RT-PCR for alpha smooth muscle actin (αSMA), collagen IA1, *TGFβ* and *MMP-2* (Fig. 7F).

These results clearly demonstrate that administration of Evasin-4 reduced disease progression in *NEMO*Δhepa mice, correlating with decreased immune cell infiltration.

Discussion

Inflammation, especially after tissue injury or contact with pathogens, is a physiological response for tissue regeneration and is particularly important for liver homeostasis. Chronic tissue injury continuously activates the immune system leading to tissue remodeling and in the liver triggers fibrogenesis and malignant transformation/growth. The role of CCL5 during this process is not fully understood.
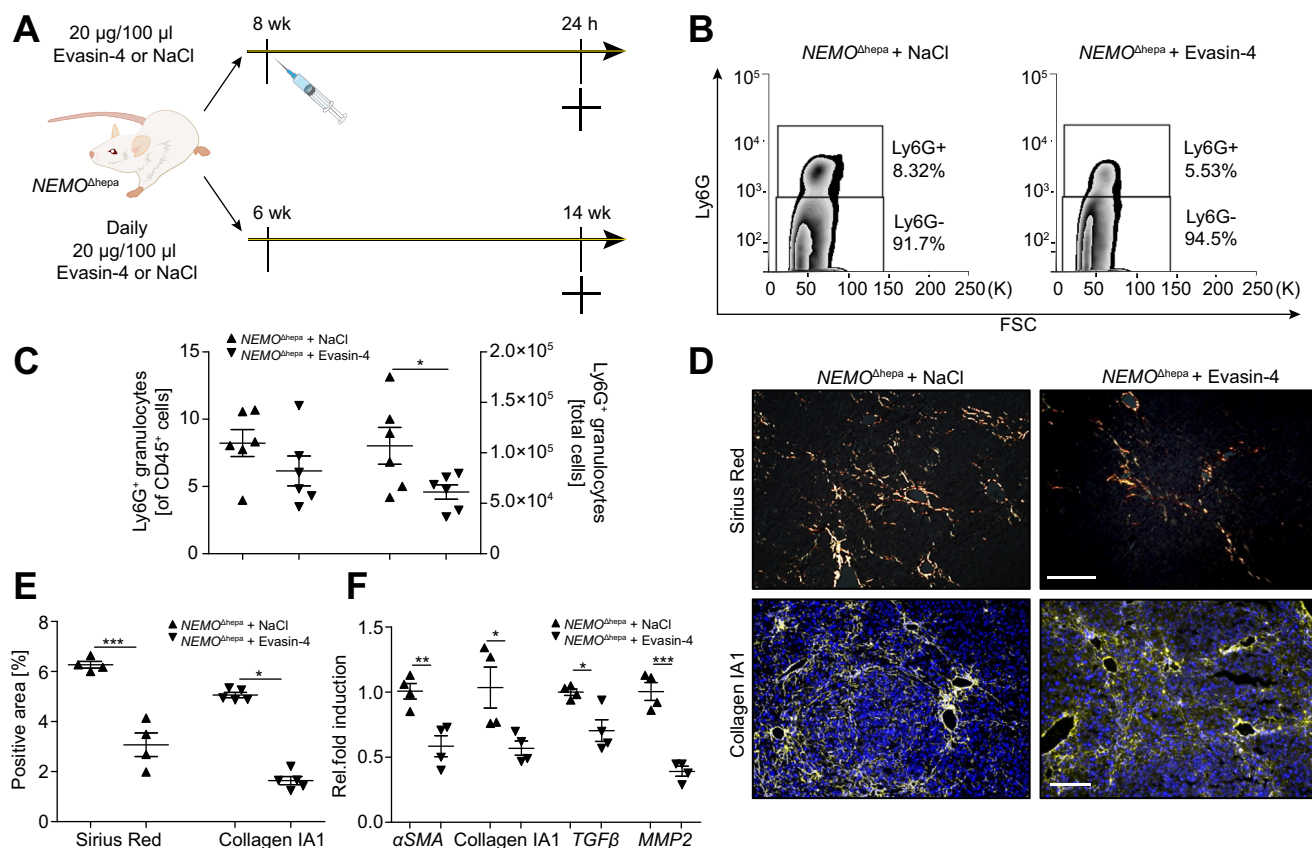
Fig. 7. Therapeutic intervention with Evasin-4 in NEMO$^{\Delta hepa}$ mice attenuates liver fibrosis. (A) Experimental setup. 8 week old NEMO$^{\Delta hepa}$ mice were injected with 20 µg/100 µl Evasin-4 or control (NaCl) and were sacrificed after 24 h (B, C). 6 week old NEMO$^{\Delta hepa}$ mice were injected daily intraperitoneal with 20 µg/100 µl Evasin-4 or control (NaCl). After 8 weeks mice were sacrificed and analyzed (D–F). (B) Total leucocytes were isolated and stained for Ly6G$^+$ granulocytes. Representative FACS plots from NEMO$^{\Delta hepa}$ treated with NaCl and NEMO$^{\Delta hepa}$ treated with Evasin-4 are shown. (C) Quantification of Ly6G$^+$ granulocytes of CD45$^+$ cells was done using FlowJo. (D) Representative images of Sirius Red (top) and collagen IA1 (bottom) stained sections. Nuclei were counterstained with DAPI. Scale bar: 200 µm. (E) Quantification of Sirius Red and collagen IA1 positive area was performed by using Image J. (F) Expression of αSMA, Collagen IA1, TGFβ and MMP2 were measured by qRT-PCR in whole liver and presented as fold induction compared with WT mice. Data are expressed as mean ± SEM from 4 mice per group. Statistical differences were detected by a 2-tailed Student's t test ($^*p$ <0.05; $^{**}p$ <0.01; $^{***}p$ = 0.001).

RANTES/CCL5 is of broad clinical importance since its increased expression has been identified in several human diseases including AIDS, cancer, atherosclerosis, asthma, transplantation, and autoimmune diseases [25]. Acute and chronic liver diseases are characterized by hepatocyte injury triggering an inflammatory and pro-fibrogenic response. Damaged hepatocytes as well as activated Kupffer cells release reactive oxygen species, as well as inflammatory mediators (e.g. CCL5 [26]) recruiting inflammatory cells to the liver, which are amplifying this process. In fact, our group provided evidence that CCL5 is strongly associated with advanced liver fibrosis with or without HCV-infection [8].

Moreover, here we show that CCL5 expression levels in CLD patients correlate with fibrosis stage and inflammation grade, especially in patients with steatosis. Importantly, we explicitly defined NPC as the major source of CCL5 in CLD patients. Additionally, CCR5 expression levels were significantly upregulated in CLD patients, whereas CCR1 and CCR3 expression were not affected.

Consequently, we asked whether CCL5 might play a crucial role in experimental inflammation-driven liver carcinogenesis and thus used the NEMO$^{\Delta hepa}$ and the Mdr2$^{-/-}$ model to address this question. Our results showed increased CCL5 expression in NEMO$^{\Delta hepa}$ and Mdr2$^{-/-}$ livers, suggesting a possible functional role for inflammation mediated HCC development. Moreover, we observed upregulation of CCR5, in contrast to CCR1 and CCR3 in NEMO$^{\Delta hepa}$ livers, indicating that most of the effects of CCL5 is mediated through CCR5 in this model. In contrast in Mdr2$^{-/-}$ livers the three receptors were not significantly upregulated, suggesting differences in the mechanisms. In NEMO$^{\Delta hepa}$ livers we determined the cell populations expressing predominantly CCR1 and CCR5 to serve as CCL5 target cells. The non-immune cell fraction showed CCR5 upregulation while CCR1 was only slightly upregulated [12]. In contrast a strong upregulation of CCR5 was found in immune cells, especially T cells, macrophages and granulocytes, suggesting that these cells are dominantly responding to increased CCL5 expression in NEMO$^{\Delta hepa}$ livers. Therefore in our further functional analysis we concentrated on NEMO$^{\Delta hepa}$ livers as they more closely reflect the receptor expression pattern as also found in human.

As CCL5 was increased during NEMO$^{\Delta hepa}$-mediated CLD, we aimed to investigate its relevance for inflammation, fibrosis and hepatocarcinogenesis. Therefore, we used a genetic approach by deleting CCL5 and generating double knockout NEMO$^{\Delta hepa}$/

Research Article

$CCL5^{-/-}$ animals. Interestingly, in $NEMO^{\Delta hepa}/CCL5^{-/-}$ mice liver injury was significantly improved compared with $NEMO^{\Delta hepa}$ mice as shown by reduced serum transaminases as well as less pronounced liver damage on histological examination. This was further supported when primary hepatocytes were isolated. Viability of $NEMO^{\Delta hepa}$ hepatocytes was significantly worse compared with $NEMO^{\Delta hepa}/CCL5^{-/-}$ hepatocytes suggesting that these cells were more severely damaged in the *in vivo* environment of $NEMO^{\Delta hepa}$ livers. In contrast, isolated primary hepatocytes of both strains in culture did not show any differences in viability and TNF response demonstrating that the inflammatory response in the liver and not the sensitivity of the hepatocyte per se is essential to explain differences in the phenotype between $NEMO^{\Delta hepa}$ and $NEMO^{\Delta hepa}/CCL5^{-/-}$ livers.

As the differences in liver damage between the two mouse strains could not be explained on the hepatocyte level, we next analyzed the inflammatory milieu and immune cell recruitment. Since CCL5 plays an active role in attracting leukocytes to inflammatory sites including T cells, macrophages, eosinophils, and basophils [11]. Loss of CCL5 reduced immune cell infiltration into $NEMO^{\Delta hepa}$ livers. Specifically, $Ly6G^+$ granulocytes, $CD11b^+/Gr1.1^+/F4/80^+$ pro-inflammatory monocytes as well as $CD4^+$ and $CD8^+$ T cells were reduced in $NEMO^{\Delta hepa}/CCL5^{-/-}$ livers. The relationship between CCL5 and $Ly6G^+$ granulocytes have been described in other tissues like in pneumonia and heart infarct [27,28]. In the present study we were thus thrilled to see that CCL5 also controls the influx of $Ly6G^+$ granulocytes in CLD.

Deletion of the CCL5 receptor *CCR5* leads to increased NK cell recruitment into the liver during ConA-induced liver injury and consequently their activation through enhanced hepatic production of CCL5 is triggered via CCR1 [29,30]. Thus, in the absence of *CCR5*, CCL5 is able to bind to other cognate receptors such as CCR1, triggering the fibrogenic response. In line with previous studies performed in our lab, genetic or pharmacological deletion of CCL5 leads to reduced fibrogenesis in three different models of liver disease, CCL_4, MCD and $NEMO^{\Delta hepa}$, confirming its potential use as a pharmacological target e.g. against NASH also in human [8,31].

Malignant growth of HCC represents the end-stage of many CLDs including the $NEMO^{\Delta hepa}$ model. Indeed, the role of CCL5 in carcinogenesis has been broadly studied in hematological malignancies and solid tumors [32], but the pro-malignant effects have only been linked to multiple melanoma and breast cancer, whereas their contribution to other malignancies remained imprecise [32].

Here we showed that *CCL5* deletion attenuates HCC progression in $NEMO^{\Delta hepa}$ mice accompanied with a reduced proliferative capacity and diminished angiogenesis. These results are consistent with previous publications suggesting that CCR5 expression is crucial for HCC progression by reducing the macrophage influx at an earlier time point. Our *in vitro* experiments demonstrated that CCL5 increases *VEGF* expression in the human HSC line Lx2, HepG2 hepatoma cells and primary murine HSCs leading to increased vessel like formation in a HUVEC based tube formation assay. This observation suggests that in the liver CCL5 via VEGF contributes to angiogenesis. Similar results have already been described for two different bone-derived tumor cell types, osteosarcoma and chondrosarcoma cells [33,34]. These results strengthen our *in vivo* results showing that $NEMO^{\Delta hepa}/CCL5^{-/-}$ tumors have a reduction in vessel formation and thus provide a direct explanation for this observation.

After our analysis suggested that NPCs in the liver and most likely immune cells are essential in mediating the CCL5-dependent effect in $NEMO^{\Delta hepa}$ livers we generated chimeric mice using BMT. These results conclusively demonstrated that immune cells expressing CCL5 derived from the hematopoietic BMT are crucial in triggering liver disease progression in $NEMO^{\Delta hepa}$ mice [8,35].

A fundamental objective in treating CLD or inflammation-driven carcinogenesis is to disrupt the interactions leading to NASH progression or HCC. Several previous promising findings using CCL5 receptor antagonism of CCR1 and/or CCR5 not only by our group (Met-CCL5) have opened new opportunities for the treatment of liver scarring in the past few years [8,36]. However, the fact that antagonism of CCR5 induces severe liver toxicity in human trials has raised concerns, and new experimental approaches need to be introduced [37]. Hence among these, targeting CCL5 via specific inhibitors might be a promising alternative approach.

Evasins, are chemokine-binding proteins identified in the blood-feeding parasitic common brown dog tick, have shown anti-inflammatory properties in experimental models of inflammatory diseases [17,38,39]. Specifically, Evasin-4 has exhibited very powerful anti-inflammatory and pro-survival properties in a post-infarction myocardial injury model [40]. Thus, we tested whether Evasin-4 might have anti-inflammatory effects in CLD. In a long-term treatment (8 weeks), Evasin-4 treated $NEMO^{\Delta hepa}$ mice developed significantly reduced liver fibrosis compared with saline injected-$NEMO^{\Delta hepa}$ mice. Furthermore Evasin-4 treatment led to a reduction of $Ly6G^+$ granulocytes. The effects of Evasin-4 were evident at the histological, biochemical, and molecular level, suggesting a profound pharmacological effect of CCL5 inhibition via Evasin-4 treatment on liver fibrogenesis.

In summary, *CCL5* deletion specifically in bone marrow derived immune cells leads to the amelioration of fibrosis and HCC progression. Pharmacologic modulation of the CCL5 pathway significantly diminished the inflammatory response and inhibited CLD progression. These results provide the rationale evidence and encourage further studies of CCL5-inhibitory strategies by using Evasins for the treatment of chronic liver injury.

Conflict of interest

The authors who have taken part in this study declared that they do not have anything to disclose regarding funding or conflict of interest with respect to this manuscript.

Authors' contributions

A.M.: experimental design; acquisition of data; analysis an interpretation of data, drafting of the manuscript; statistical analysis; N. K., S.A.Y, A.B and R.S.: acquisition of data; critical revision of

the manuscript; J.R., H.W.Z. and A.P. material support; critical revision of the manuscript; F.J.C.: critical revision of the manuscript; C.T.: study concept and design; study supervision; critical revision of the manuscript for important intellectual content.

Supplementary data

References

Author names in bold designate shared co-first authorship

[1] Sun B, Karin M. Inflammation and liver tumorigenesis. Front Med 2013;7:242–254.

[2] Parkin DM, Bray F, Ferlay J, Pisani P. Estimating the world cancer burden: Globocan 2000. Int J Cancer 2001;94:153–156.

[3] Coussens LM, Werb Z. Inflammation and cancer. Nature 2002;420:860–867.

[4] Karin M. Nuclear factor-kappaB in cancer development and progression. Nature 2006;441:431–436.

[5] Mantovani A, Allavena P, Sica A, Balkwill F. Cancer-related inflammation. Nature 2008;454:436–444.

[6] Marra F, Tacke F. Roles for chemokines in liver disease. Gastroenterology 2014;147:577–594 e571.

[7] Schall TJ, Jongstra J, Dyer BJ, Jorgensen J, Clayberger C, Davis MM, et al. A human T cell-specific molecule is a member of a new gene family. J Immunol 1988;141:1018–1025.

[8] Berres ML, Koenen RR, Rueland A, Zaldivar MM, Heinrichs D, Sahin H, et al. Antagonism of the chemokine Ccl5 ameliorates experimental liver fibrosis in mice. J Clin Invest 2010;120:4129–4140.

[9] Devergne O, Marfaing-Koka A, Schall TJ, Leger-Ravet MB, Sadick M, Peuchmaur M, et al. Production of the RANTES chemokine in delayed-type hypersensitivity reactions: involvement of macrophages and endothelial cells. J Exp Med 1994;179:1689–1694.

[10] Schwabe RF, Bataller R, Brenner DA. Human hepatic stellate cells express CCR5 and RANTES to induce proliferation and migration. Am J Physiol Gastrointest Liver Physiol 2003;285:G949–G958.

[11] **Bacon KB**, **Premack BA**, Gardner P, Schall TJ. Activation of dual T cell signaling pathways by the chemokine RANTES. Science 1995;269:1727–1730.

[12] Seki E, De Minicis S, Gwak GY, Kluwe J, Inokuchi S, Bursill CA, et al. CCR1 and CCR5 promote hepatic fibrosis in mice. J Clin Invest 2009;119:1858–1870.

[13] Barashi N, Weiss ID, Wald O, Wald H, Beider K, Abraham M, et al. Inflammation-induced hepatocellular carcinoma is dependent on CCR5 in mice. Hepatology 2013;58:1021–1030.

[14] Yang X, Lu P, Fujii C, Nakamoto Y, Gao JL, Kaneko S, et al. Essential contribution of a chemokine, CCL3, and its receptor, CCR1, to hepatocellular carcinoma progression. Int J Cancer 2006;118:1869–1876.

[15] Luedde T, Beraza N, Kotsikoris V, van Loo G, Nenci A, De Vos R, et al. Deletion of NEMO/IKKgamma in liver parenchymal cells causes steatohepatitis and hepatocellular carcinoma. Cancer Cell 2007;11:119–132.

[16] Beraza N, Malato Y, Sander LE, Al-Masaoudi M, Freimuth J, Riethmacher D, et al. Hepatocyte-specific NEMO deletion promotes NK/NKT cell- and TRAIL-dependent liver damage. J Exp Med 2009;206:1727–1737.

[17] Déruaz M, Frauenschuh A, Alessandri AL, Dias JM, Coelho FM, Russo RC, et al. Ticks produce highly selective chemokine binding proteins with antiinflammatory activity. J Exp Med 2008;205:2019–2031.

[18] Déruaz M, Bonvin P, Severin IC, Johnson Z, Krohn S, Power CA, et al. Evasin-4, a tick-derived chemokine-binding protein with broad selectivity can be modified for use in preclinical disease models. FEBS J 2013;280:4876–4887.

[19] Beraza N, Ludde T, Assmus U, Roskams T, Vander Borght S, Trautwein C. Hepatocyte-specific IKK gamma/NEMO expression determines the degree of liver injury. Gastroenterology 2007;132:2504–2517.

[20] Makino Y, Cook DN, Smithies O, Hwang OY, Neilson EG, Turka LA, et al. Impaired T cell function in RANTES-deficient mice. Clin Immunol 2002;102:302–309.

[21] Zimmermann HW, Seidler S, Nattermann J, Gassler N, Hellerbrand C, Zernecke A, et al. Functional contribution of elevated circulating and hepatic non-classical CD14CD16 monocytes to inflammation and human liver fibrosis. PLoS One 2010;5 e11049.

[22] Cubero FJ, Zhao G, Nevzorova YA, Hatting M, Al Masaoudi M, Verdier J, et al. Haematopoietic cell-derived Jnk1 is crucial for chronic inflammation and carcinogenesis in an experimental model of liver injury. J Hepatol 2015;62:140–149.

[23] Nussenbaum F, Herman IM. Tumor angiogenesis: insights and innovations. J Oncol 2010;2010 132641.

[24] Frauenschuh A, Power CA, Déruaz M, Ferreira BR, Silva JS, Teixeira MM, et al. Molecular cloning and characterization of a highly selective chemokine-binding protein from the tick Rhipicephalus sanguineus. J Biol Chem 2007;282:27250–27258.

[25] Krensky AM, Ahn YT. Mechanisms of disease: regulation of RANTES (CCL5) in renal disease. Nat Clin Pract Nephrol 2007;3:164–170.

[26] Scott MJ, Chen C, Sun Q, Billiar TR. Hepatocytes express functional NOD1 and NOD2 receptors: a role for NOD1 in hepatocyte CC and CXC chemokine production. J Hepatol 2010;53:693–701.

[27] Lee CS, Yi EH, Lee JK, Won C, Lee YJ, Shin MK, et al. Simvastatin suppresses RANTES-mediated neutrophilia in polyinosinic-polycytidylic acid-induced pneumonia. Eur Respir J 2013;41:1147–1156.

[28] Montecucco F, Braunersreuther V, Lenglet S, Delattre BM, Pelli G, Buatois V, et al. CC chemokine CCL5 plays a central role impacting infarct size and post-infarction heart failure in mice. Eur Heart J 2012;33:1964–1974.

[29] Ajuebor MN, Aspinall AI, Zhou F, Le T, Yang Y, Urbanski SJ, et al. Lack of chemokine receptor CCR5 promotes murine fulminant liver failure by preventing the apoptosis of activated CD1d-restricted NKT cells. J Immunol 2005;174:8027–8037.

[30] Moreno C, Gustot T, Nicaise C, Quertinmont E, Nagy N, Parmentier M, et al. CCR5 deficiency exacerbates T-cell-mediated hepatitis in mice. Hepatology 2005;42:854–862.

[31] Nellen A, Heinrichs D, Berres ML, Sahin H, Schmitz P, Proudfoot AE, et al. Interference with oligomerization and glycosaminoglycan binding of the chemokine CCL5 improves experimental liver injury. PLoS One 2012;7 e36614.

[32] Aldinucci D, Colombatti A. The inflammatory chemokine CCL5 and cancer progression. Mediators Inflamm 2014;2014 292376.

[33] Liu GT, Chen HT, Tsou HK, Tan TW, Fong YC, Chen PC, et al. CCL5 promotes VEGF-dependent angiogenesis by down-regulating miR-200b through PI3K/Akt signaling pathway in human chondrosarcoma cells. Oncotarget 2014;5:10718–10731.

[34] Wang SW, Liu SC, Sun HL, Huang TY, Chan CH, Yang CY, et al. CCL5/CCR5 axis induces vascular endothelial growth factor-mediated tumor angiogenesis in human osteosarcoma microenvironment. Carcinogenesis 2015;36:104–114.

[35] Koenen RR, von Hundelshausen P, Nesmelova IV, Zernecke A, Liehn EA, Sarabi A, et al. Disrupting functional interactions between platelet chemokines inhibits atherosclerosis in hyperlipidemic mice. Nat Med 2009;15:97–103.

[36] Pérez-Martínez L, Pérez-Matute P, Aguilera-Lizarraga J, Rubio-Mediavilla S, Narro J, Recio E, et al. Maraviroc, a CCR5 antagonist, ameliorates the development of hepatic steatosis in a mouse model of non-alcoholic fatty liver disease (NAFLD). J Antimicrob Chemother 2014;69:1903–1910.

[37] Nichols WG, Steel HM, Bonny T, Adkison K, Curtis L, Millard J, et al. Hepatotoxicity observed in clinical trials of aplaviroc (GW873140). Antimicrob Agents Chemother 2008;52:858–865.

[38] Vieira AT, Fagundes CT, Alessandri AL, Castor MG, Guabiraba R, Borges VO, et al. Treatment with a novel chemokine-binding protein or eosinophil lineage-ablation protects mice from experimental colitis. Am J Pathol 2009;175:2382–2391.

[39] Castor MG, Rezende B, Resende CB, Alessandri AL, Fagundes CT, Sousa LP, et al. The CCL3/macrophage inflammatory protein-1alpha-binding protein evasin-1 protects from graft-versus-host disease but does not modify graft-versus-leukemia in mice. J Immunol 2010;184:2646–2654.

[40] Braunersreuther V, Montecucco F, Pelli G, Galan K, Proudfoot AE, Belin A, et al. Treatment with the CC chemokine-binding protein Evasin-4 improves post-infarction myocardial injury and survival in mice. Thromb Haemost 2013;110:807–825.

Cancer